Pion-nucleus scattering at 800 MeV/c

Masaki Arima
Department of Physics, Faculty of Science, University of Tokyo, Bunkyo-ku, Tokyo 113, Japan

Keiichi Masutani
Department of Physics, Yamanashi University, Kofu 400, Japan

Ryoichi Seki
Department of Physics, California State University, Northridge, California 91330
and W. K. Kellogg Radiation Laboratory, California Institute of Technology, Pasadena, California 91125
(Received 31 October 1990)

Elastic π-^{12}C scattering at 800 MeV/c is investigated by the means of the Glauber theory and the optical-potential model. Various effects associated with the first-order potential are carefully examined as well as higher-order effects of nuclear correlations and pion absorption. A clear discrepancy persists between the calculation and the data. The calculation is extended to the single- and double-charge-exchange processes at 800 MeV/c.

I. INTRODUCTION

The π-nucleus interaction above the Δ resonance, say, above 500 MeV/c, is a relatively unexplored field in nuclear physics. Only some exploratory works have been done experimentally and theoretically. In the near future, however, we will be in a better position to study the subject when high-intensity π beams of new higher-energy facilities become available at LAMPF (the PILAC Project), at TRIUMF (the KAON Project), and at KEK (the Japanese Hadron Project), in addition to the existing facilities at Brookhaven National Laboratory and KEK.

Elastic π-nucleus scattering data above the Δ resonance are scarce at present. In this theoretical work, we mostly examine the 800 MeV/c (673 MeV in the laboratory system) data obtained at Brookhaven National Laboratory [1] and briefly examine recent 400 and 500 MeV data from LAMPF [2] for comparison. The Brookhaven data include elastic and inelastic cross sections for $\pi^{\pm}$-^{12}C and ^{40}Ca scattering, but in this work we concentrate on the elastic ^{12}C scattering. As will be discussed later (in Sec. VI), we verify that our results are similar for scattering from both nuclei. Preliminary results have been briefly reported previously [3].

The πN interaction at 800 MeV/c differs from the interaction at and below the Δ resonance, and this difference brings about a difference in the π-nuclear interaction in the two energy regions. In the following we list the prominent features of the pion kinematics and dynamics at this energy since they will play an important, sometimes decisive, role in our investigation.

(1) The wavelength of incident pion is short, nearly $\frac{1}{4}$ fm at 800 MeV/c, and the momentum transfer involved in scattering also corresponds to a short distance, for example, about 0.5 fm at the scattering angle of 30°. As a consequence of this kinematics, short-range nuclear phenomena become relatively significant in the π-nuclear interaction.

(2) The πN total cross section is much smaller (about 30 mb) than those around the Δ resonance (about 150 mb). In fact, the πN cross section is about twice the magnitude of the K^+N cross section, while the K^+ is known to be the most weakly interacting hadron probe. The pion thus has a long mean free path of about 2 fm in nuclei, which implies a smaller number of multiple scattering to occur.

(3) The πN scattering amplitude is reasonably well peaked in the forward direction in the laboratory coordinate system, in fact, a little sharper than at the Δ-resonance energy. This allows us to apply the Glauber theory to π-nucleus scattering. Note that because of the large incident-pion momentum, the peak appears to be wide as a function of the *momentum transfer,* in fact, wider than that of the nuclear form factor, as is seen in Appendix A. Consequently, the shape of the near-forward π-nucleus cross section follows the nuclear form factor.

(4) While the Δ resonance of the isospin $I=\frac{3}{2}$ dominates the πN interaction below 500 MeV/c, many resonances contribute to the interaction above 500 MeV/c. Around 800 MeV/c, however, only a few $I=\frac{1}{2}$ resonances [$N(1440)$, $N(1520)$, and $N(1535)$] appear. The difference between $I=\frac{3}{2}$ and $\frac{1}{2}$ has an important consequence: For example, for the incident π^+, the Δ is formed predominantly with the proton, but the $I=\frac{1}{2}$ resonances are formed only with the neutron. The resonances in this high-energy region have large inelasticity and decay widths with appreciable backgrounds, and are thus expected to be less dominant than the Δ below 500 MeV/c. Note that the large inelasticity is mostly due to pion production.

Below 500 MeV/c, the Δ dominance provides a useful theoretical method of the isobar-hole model. An obvious

question is whether the method should also be applied to this problem. Apart from technical complications arising from several almost overlapping resonances, the large inelasticity and decay widths with appreciable backgrounds do not appear to be encouraging signs for the model to be a useful means at this energy. At the same time, (1) and (2) above suggest a multiple-scattering series to converge rapidly. Accordingly, we have decided to apply in this first investigation the method of multiple scattering, using two formalisms, the Glauber theory [4] and the optical-potential model [5].

The formalisms were originally constructed basically for nuclear scattering by the nucleon and would require modification for the pion because of special medium corrections stemming from its bosonic nature. It is conceivable that the corrections would be too extensive for the formalisms to be suitable in this energy range. Here, however, we assume the formalisms to be suitable and include in them the obvious medium corrections (the Pauli correlation, the nuclear binding effect, and the dynamical two-nucleon correlation) and the contribution from pion absorption. Other more intricate corrections are left for our future work, in which we plan to address the question of suitability of the isobar-hole model at this energy. Within this framework we apply the formalisms as carefully as possible: We use the two similar formalisms to ensure reliability of our findings. As we proceed to include higher-order effects in the expansion, we carefully compare our results with the data at each step of the calculation. In this way we hope not to overlook, by prejudice from low energies, any new important effect at this new energy.

In Sec. II we first describe how we apply two formalisms in our problem. Results of the lowest-order approximation in the formalisms are shown and are compared with the data in Sec. III. The objectives of this calculation are to find out, at this energy region, the validity of the Glauber theory and the significance of various effects associated with the lowest-order approximation. Section IV includes a microscopic examination of effects beyond the lowest-order impulse approximation, the effects of nuclear correlations, and π absorption. We extend the calculation to charge-exchange reactions with the isobaric-analog states in Sec. V. Summary and discussions of our work are given in Sec. VI. Appendixes include brief sketches of how we treat the πN amplitudes, the nuclear center-of-mass correction, and the pion absorption.

Our calculation basically follows the standard procedure, which is well described, for example, in a comprehensive treatment of pion-nuclear physics below Δ by Eisenberg and Koltun [6]. Suitable to this high energy, however, we apply and modify the procedure, and sometimes introduce some new treatment. Since this is an important aspect of our work, in what follows we will describe our calculations somewhat more carefully, and perhaps more in detail, than we would do otherwise.

II. MULTIPLE-SCATTERING EXPANSION IN TWO FORMALISMS

In this section we describe how we use two formalisms based on the multiple-scattering expansions. Our usage is basically the standard one, but care has been taken to apply appropriate coordinate transformations in their application. We find that this aspect is quite important in the treatment of the relativistic pion. Without such care, higher-order corrections, which will be examined in Sec. IV, would have been pointless.

A. Glauber theory

The π-nucleus scattering amplitude in the Glauber theory is formally written in the π-nucleus center-of-mass (c.m.) system as [4]

$$G(\mathbf{Q})=\frac{k}{2\pi i}\int d^2b\, e^{i\mathbf{b}\cdot\mathbf{Q}}\int d^3r_1\cdots d^3r_A\,\psi_0^\dagger(\mathbf{r}_1,\ldots,\mathbf{r}_A)\left[\prod_j^A[1-\Gamma(\mathbf{b}-\mathbf{s}_j)]-1\right]\psi_0(\mathbf{r}_1,\ldots,\mathbf{r}_A)\delta\left[A^{-1}\sum_j^A\mathbf{r}_j\right], \tag{1}$$

where $\psi_0(\mathbf{r}_1,\ldots,\mathbf{r}_A)$ is the ground-state wave function of the target nucleus consisting of A nucleons, the coordinate of the jth nucleon being $\mathbf{r}_j$. The incident-pion momentum and the momentum transfer are denoted by $\mathbf{k}$ and $\mathbf{Q}$, respectively. The impact parameter is $\mathbf{b}$, and $\mathbf{s}_j$ is a component of $\mathbf{r}_j$ perpendicular to $\mathbf{k}$. The c.m. of the nucleus is set at the origin by the delta function, and all coordinates are measured with respect to this nuclear c.m.

$\Gamma(\mathbf{b})$ is the profile function for a nucleon and is expressed in terms of the πN scattering amplitude in the πN c.m. system $f(q)$ as

$$\Gamma(\mathbf{b})=\frac{1}{2\pi i\kappa}\int d^2q\, e^{-i\mathbf{q}\cdot\mathbf{b}}f(q)\,, \tag{2}$$

where the subscript specifying the nucleon [such as j as in Eq. (1)] is suppressed for simplicity. Here κ is the magnitude of the πN relative momentum, and $\mathbf{q}$ is the momentum transfer in the πN scattering. Note that $f(q=0)/\kappa$ is a Lorentz-invariant quantity, as is evident from the optical theorem. In fact, $f(q)/\kappa$ and $\Gamma(\mathbf{b})$ can be shown to be approximately invariant in the Glauber theory [7].

The nuclear wave function ψ_0 is a complicated, many-body function, especially in a relativistic treatment, and becomes unmanageably complicated when the c.m. motion is incorporated through the delta function in Eq. (1). For practical purposes we make here the major approximation in our calculation, treating the nucleus nonrelativistically while treating the pion to obey the relativistic kinematics. In this work we use the Slater determinant of the single-particle, shell-model wave functions as the nonrelativistic wave function:

$$\psi_{\rm SM}(\mathbf{r}'_1,\mathbf{r}'_2,\ldots,\mathbf{r}'_A)=\frac{1}{\sqrt{A!}}\sum_{\{i,j,\ldots,k\}}\epsilon_{i,j,\ldots,k}\phi_i(\mathbf{r}'_1)\phi_j(\mathbf{r}'_2)\cdots\phi_k(\mathbf{r}'_A)\ , \tag{3}$$

where the ϕ_i's are harmonic-oscillator (HO) wave functions. The shell-model space is restricted only to the $s_{1/2}$ and $p_{3/2}$ states for ^{12}C, and $\epsilon_{i,j,\ldots,k}$ is the sign of a permutation $\{i,j,\ldots,k\}$ for the nucleon states. Since the $\mathbf{r}'$'s in Eq. (3) are measured with respect to the center of the shell-model potential, the c.m. motion must be corrected for, when we use $\psi_{\rm SM}(\mathbf{r}'_1,\mathbf{r}'_2,\ldots,\mathbf{r}'_A)$ in place of $\psi_0(\mathbf{r}_1,\ldots,\mathbf{r}_A)$ in Eq. (1). The use of the HO wave functions simplifies the correction. As shown in Appendix B, the correction amounts to a simple, multiplicative factor to the amplitude [8],

$$G(\mathbf{Q})=\exp\left[\frac{Q^2a_0^2}{4A}\right]\times[\text{Eq.(1) without the }\delta\text{ function}]\ , \tag{4}$$

where all coordinates in Eq. (1) are now measured with respect to the center of the shell-model potential. The HO parameter a_0 is taken to be 1.61 fm. This value is obtained from the nuclear charge density by including the c.m. correction and by unfolding the nucleon form factor [9]. The charge density used has the form

$$\rho_{\rm ch}(r)=\rho_0\left[1+\alpha\left[\frac{r}{a}\right]^2\right]\exp\left[-\left[\frac{r}{a}\right]^2\right]\ , \tag{5}$$

with $a=1.672$ fm and $\alpha=1.15$, so as to fit high-energy, electron-scattering data [10]. As the nucleon form factor, we use the (square) dipole form [11]

$$\tilde{\rho}(q^2)=(1+q^2/\tilde{q}^{\,2})^{-2}\ , \tag{6}$$

with $\tilde{q}=4.26$ fm^{-1}.

Equation (1) is now expressed as the standard form of a multiple-scattering series,

$$\begin{aligned}G(\mathbf{Q})=\exp\left[\frac{Q^2a_0^2}{4A}\right]\frac{k}{2\pi i}\int d^2b\,e^{i\mathbf{b}\cdot\mathbf{Q}}\int d^3r_1\cdots d^3r_A\,\psi^\dagger_{\rm SM}(\mathbf{r}_1,\ldots,\mathbf{r}_A)\\ \times\left[-\sum_{i=1}^{A}\Gamma(\mathbf{b}-\mathbf{s}_i)+\sum_{i<j}^{A}\Gamma(\mathbf{b}-\mathbf{s}_i)\Gamma(\mathbf{b}-\mathbf{s}_j)\right.\\ \left.+\cdots+(-)^A\Gamma(\mathbf{b}-\mathbf{s}_1)\Gamma(\mathbf{b}-\mathbf{s}_2)\cdots\Gamma(\mathbf{b}-\mathbf{s}_A)\right]\psi_{\rm SM}(\mathbf{r}_1,\ldots,\mathbf{r}_A)\ ,\end{aligned} \tag{7}$$

where all possible nuclear states must be considered between adjacent Γ functions. For the sake of simplicity, in Eq. (7) and hereafter, we suppress the primes on the coordinates measured with respect to the center of the shell-model potential. Equation (7) can be written as

$$\begin{aligned}G(\mathbf{Q})&=\exp\left[\frac{Q^2a_0^2}{4A}\right]\frac{k}{2\pi i}\int d^2b\,e^{i\mathbf{b}\cdot\mathbf{Q}}[\det(1-\Gamma_{i,j})-1]\\ &=\exp\left[\frac{Q^2a_0^2}{4A}\right]\frac{k}{2\pi i}\int d^2b\,e^{i\mathbf{b}\cdot\mathbf{Q}}\left[-\sum_{i}^{A}\Gamma_{i,i}+\sum_{i<j}^{A}(\Gamma_{i,i}\Gamma_{j,j}-\Gamma_{i,j}\Gamma_{j,i})+\cdots\right]\ ,\end{aligned} \tag{8}$$

where

$$\Gamma_{i,j}=\int d^3r\,\phi_i^\dagger(\mathbf{r})\Gamma(\mathbf{b}-\mathbf{s})\phi_j(\mathbf{r})\ . \tag{9}$$

The determinants encompass all nuclear states considered.

The Γ's are actually vector and/or isovector operators and do not commute with each other. Equations (1) and (7), however, assume otherwise and are approximated expressions. The correct expressions for them are quite complicated when the requirement of the Glauber theory is also correctly incorporated so that only near-forward scattering is taken into account. As will be described in Sec. III B, we find the effects of the spin- and isospin-flip amplitudes to be negligible. Accordingly, we will use Eq. (8) in our Glauber calculations. Note that the evaluation of Eq. (8) is simplified because of our limited shell-model space and the rapid convergence of the series at this energy.

If we make a further approximation of neglecting Pauli correlation and dependence on the single-particle-state quantum numbers, the series can be summed and Eq. (8) becomes a simple expression:

$$G(\mathbf{Q})\approx\exp\left[\frac{Q^2a_0^2}{4A}\right]\frac{k}{2\pi i}\int d^2b\, e^{i\mathbf{b}\cdot\mathbf{Q}}\left[\int\prod_j^A[1-\Gamma(\mathbf{b}-\mathbf{s}_j)]\rho_j(\mathbf{r}_j)d^3r_j-1\right]$$

$$\approx\exp\left[\frac{Q^2a_0^2}{4A}\right]\frac{k}{2\pi i}\int d^2b\, e^{i\mathbf{b}\cdot\mathbf{Q}}\left[\left[\int[1-\Gamma(\mathbf{b}-\mathbf{s})]\rho(\mathbf{r})d^3r\right]^A-1\right], \tag{10}$$

where $\rho_j(\mathbf{r})=|\phi_j(\mathbf{r})|^2\approx\sum_k|\phi_k(\mathbf{r})|^2/A=\rho(\mathbf{r})$. Equation (10) is easily evaluated and is useful, for example, for examining the convergence of the multiple-scattering series.

Note that, as is well known [4], one can see the close relation between the multiple-scattering expansions in the Glauber theory and in the optical-potential model, through a simplified expression such as Eq. (10): Let us define the phase-shift function $\chi(\mathbf{b})$ as

$$\exp[i\chi(\mathbf{b})]=\left[\int d^3r[1-\Gamma(\mathbf{b}-\mathbf{s})]\rho(\mathbf{r})\right]^A. \tag{11}$$

For large A, $\chi(\mathbf{b})$ becomes

$$\chi(\mathbf{b})\approx iA\int d^3r\,\Gamma(\mathbf{b}-\mathbf{s})\rho(\mathbf{r})\,. \tag{12}$$

We see that $\chi(\mathbf{b})$ gives essentially the same results as the lowest-order optical potential with the eikonal approximation.

Before closing this section, let us describe $f(q)$ used in this work. Though the nuclear form factor suppresses the large q contribution of the πN amplitude, we use the partial-wave expansion of the amplitude, avoiding approximated forms such as a Gaussian form [12], in order to ensure accuracy of our calculation. We mostly use Höhler's πN phase shifts up to h wave ($L=5$) [13], and use Cutkosky *et al.*'s phase shifts [14] for comparison. For completeness we describe in Appendix A how we compute the πN amplitude $f(q)$ from the phase shifts.

One more note: For simplicity, we include no Coulomb interaction in our Glauber calculation. The interaction is included in our optical-potential calculation (discussed in the following subsection), so that serious comparison with the data will be made using an optical-model result.

B. Optical potential

As is discussed in Appendix A, our πN scattering amplitude is a complicated function of the momentum transfer. The only viable way to carry out the optical-potential calculation is to solve the Lippmann-Schwinger equation in the momentum space. The equation for the first-order optical potential $V_{\rm opt}^{(1)}(E)$ is written as

$$\langle\mathbf{k}',0|T'(E)|\mathbf{k},0\rangle=\langle\mathbf{k}',0|V_{\rm opt}^{(1)}(E)|\mathbf{k},0\rangle+\int\frac{d^3k''}{(2\pi)^3}\frac{\langle\mathbf{k}',0|V_{\rm opt}^{(1)}(E)|\mathbf{k}'',0\rangle\langle\mathbf{k}'',0|T'(E)|\mathbf{k},0\rangle}{E-(m_\pi^2+k''^2)^{1/2}-(m_A^2+k''^2)^{1/2}+i\epsilon}\,, \tag{13}$$

where m_π and m_A are the π and nuclear masses, respectively, and 0 means the ground state of the nucleus. The π-nucleus t matrix $T(E)$ is obtained from $T(E)=[A/(A-1)]T'(E)$. In order to solve the equation, we use a computer program PIPIT3, written by Eisenstein and Tabakin [15]. The program is a scattering-problem solver in momentum space, using the matrix-inversion method [16]. We make the following modifications to it that are suitable to our problem in this higher energy: (1) the use of the Höhler's phase shift up to the h-wave πN amplitude and (2) the increase of the π-nucleus partial waves to about 25. Note that $kR\approx12$, where R is the nuclear radius. Our modifications are straightforward, but are found to be nontrivial in order to ensure numerical accuracy.

The optical potential in the lowest-order impulse approximation is of the t-ρ form,

$$\langle\mathbf{k}',0|V_{\rm opt}^{(1)}(E)|\mathbf{k},0\rangle$$
$$=(A-1)\langle0|\exp(-i\mathbf{q}\cdot\mathbf{r})|0\rangle\langle\mathbf{k}'|t(e)|\mathbf{k}\rangle$$
$$=(A-1)\tilde\rho(\mathbf{q})\langle\mathbf{k}'|t(e)|\mathbf{k}\rangle\,, \tag{14}$$

in terms of the off-mass-shell, πN t-matrix element in the π-nucleus c.m. coordinate system $\langle\mathbf{k}'|t(e)|\mathbf{k}\rangle$, where e is the πN total energy in the πN c.m. system. Here $\mathbf{q}=\mathbf{k}'-\mathbf{k}$, and $\tilde\rho(\mathbf{q})$ is the nuclear form factor. Note that the kinematics used here corresponds to a frozen approximation, each nucleon being fixed in the nucleus, or the nucleon momentum $\mathbf{p}=-\mathbf{k}/A$ in the π-nucleus c.m. frame.

The off-mass-shell, t-matrix element is then constructed from the on-mass-shell element $\langle\kappa_0'|\tilde t(e)|\kappa_0\rangle$ [17]:

$$\langle\mathbf{k}'|t(e)|\mathbf{k}\rangle=\gamma\langle\kappa'|\tilde t(e)|\kappa\rangle$$
$$=\gamma\frac{g(\kappa')g(\kappa)}{g(\kappa_0)^2}\langle\kappa_0'|\tilde t(e)|\kappa_0\rangle\,. \tag{15}$$

Here

$$\gamma=\left[\frac{E_\pi(\kappa')E_\pi(\kappa)E_N(\kappa)E_N(\kappa')}{E_\pi(\mathbf{k})E_\pi(\mathbf{k}')E_N(\mathbf{p})E_N(\mathbf{p}-\mathbf{q})}\right]^{1/2}, \tag{16}$$

where E_π and E_N are the pion and nucleon total energies

for the momentum labeled, respectively. Equation (15) consists of a few steps: First, we transform the coordinates through the kinematic factor γ from the π-nucleus c.m. system to the πN c.m. system; in terms of the momenta, from $\mathbf{k}'$ and $\mathbf{k}$ to κ' and κ. Note that $\langle \kappa' | \tilde{t}(e) | \kappa \rangle$ thus constructed is an off-mass-shell πN amplitude. Second, we express this off-shell amplitude in terms of the πN on-shell amplitude through the g functions; the momenta κ' and κ are changed to κ_0' and κ_0. The last set of the momenta κ_0 and κ_0' satisfies the on-mass-shell relation in the πN c.m. coordinate system, $e=(\kappa_0^2+m_\pi^2)^{1/2}+(\kappa_0^2+m_N^2)^{1/2}$ with $|\kappa_0|=|\kappa_0'|$.

The on-mass-shell, t-matrix element is related to the πN scattering amplitude in the πN c.m. coordinate system $f(\mathbf{q}_0)$ as

$$\langle \kappa_0' | \tilde{t}(e) | \kappa_0 \rangle = -2\pi \frac{E_\pi(\kappa_0)+E_N(\kappa_0)}{E_\pi(\kappa_0)E_N(\kappa_0)} f(\mathbf{q}_0) , \quad (17)$$

where $\mathbf{q}_0=\kappa_0'-\kappa_0$. As in the case of Glauber theory, $f(\mathbf{q}_0)$ is written as a series of partial waves in the way described in Appendix A. Equation (13) is reduced to a one-dimensional form after performing the angle integral of d^3k'' analytically by expanding the t matrix as

$$\langle \mathbf{k}',0|T'(E)|\mathbf{k},0\rangle = 16\pi^2 \sum_{lm} \langle k',0|T'(E)|k,0\rangle Y_{lm}^*(\hat{k}')Y_{lm}(\hat{k}) . \quad (18)$$

The resulting integral equation is solved using PIPIT3. Note that the program includes the Coulomb interaction generated by the uniformly charged sphere, using the method of Vincent and Phatak [18]. We use the nuclear charge density of Eq. (5) to generate the nuclear form factor $\tilde{\rho}(\mathbf{q})$. The charge density includes the finite nucleon size [Eq. (6)], which must be removed. In this work we always unfold the nucleon form factor, unless we state otherwise.

III. LOWEST-ORDER RESULTS

A. Comparison of two formalisms

The two formalisms which we use are similar, but are based on different approximation schemes and can provide different insights into the problem. For example, the Glauber theory uses the on-shell πN amplitude and assumes small-angle scattering from the outset, but gives a vivid illustrative description of the scattering. Validity of these restrictions in our problem can be verified by comparing with the results of the optical-potential model. Utility of the two formalisms is thus clearly enhanced by comparing their results side by side. Once their validity is established, each can be used for calculations more advantageous to the formalism.

We first compare the differential cross sections by the two formalisms in the lowest-order impulse approximation. Equation (8) is used for the Glauber theory, and Eqs. (13)–(18) are for the optical-potential model. Note that, as stated previously, the Coulomb interaction is not included in the Glauber calculation. Figure 1 shows that the cross sections agree with each other over the momentum transfer examined, except for around the first minimum ($\sim 25°$), where the Glauber theory gives a deeper dip than that given by the optical-potential model. The origin of the difference is under further investigation. We conclude that, except for the magnitudes at dips, the two formalisms yield similar and reliable results.

Since the Glauber theory provides us an illustrative description of pion scattering in nuclei, we examine explicitly the contribution from each multiple-scattering term. Figure 2 shows the contributions from various terms in Eq. (8). We see that the multiple-scattering series converges in the fourth-scattering term. The convergence agrees with our expectation based on the geometrical argument (the nuclear diameter)/(the pion

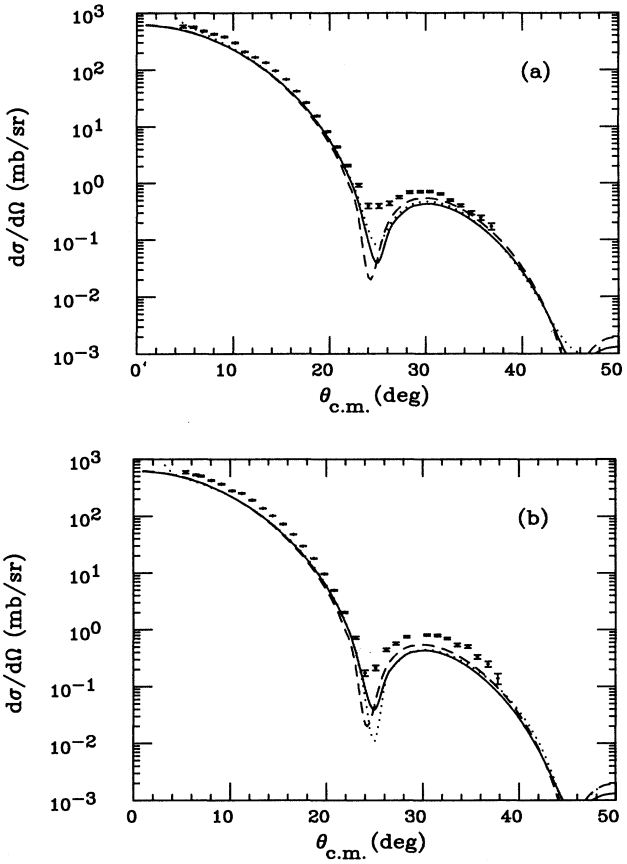

FIG. 1. (a) π^+-^{12}C elastic differential cross sections at 800 MeV/c. The dashed curve is calculated using Eq. (8) of the Glauber theory, in which the multiple-scattering series are summed, the Slater-determinant nuclear wave function is used, and the Coulomb interaction is not included. The dotted and solid curves are obtained by the first-order optical potential with and without the Coulomb interaction, using a slightly modified PIPIT3 (Ref. [15], and see text). In these lowest-order calculations, the nucleon form factor is unfolded from the nuclear form factor and the c.m. motion of the nucleus is corrected. The data are taken from Ref. [1]. (b) π^--^{12}C elastic differential cross sections at 800 MeV/c. All curves are calculated in the same way as in (a).

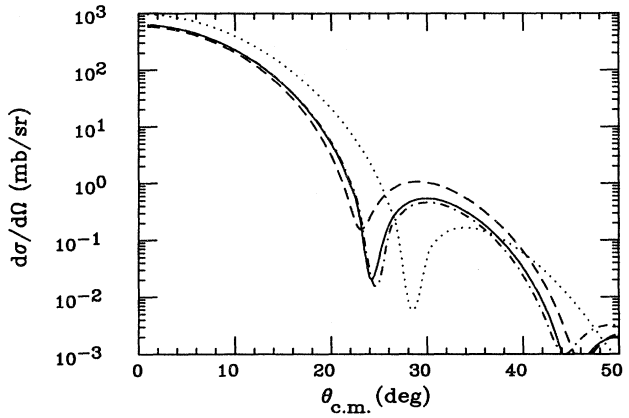

FIG. 2. Decomposition of the multiple-scattering series in the Glauber theory as given in Eq. (8) for π-^{12}C elastic scattering. The dotted curve is the contribution from the single scattering. The dashed curve is the sum of the single- and double-scattering contributions. The dot-dashed curve includes all contributions up to the triple scattering, and the solid curve up to the quadruple scattering. The solid curve here corresponds to the dashed curve in Fig. 1.

mean free path) ≈ 3. Note that the contributions from the second- and third-scattering terms are not negligible even near forward and are responsible for generating the first minimum by interference.

For completeness we examine the approximate form of the Glauber theory [Eqs. (10) and (12)]. Figure 3 shows the cross sections using the Slater-determinant form of Eq. (8), those using the density form as in Eq. (10), and those with the phase-shift function at the large-A limit [Eq. (12)]. The difference among them is seen to be at most a few percent. The antisymmetrization (Pauli correlation) effect is found to be small, and the large-A limit is also a good approximation to the full Glauber-theory calculation of Eq. (8).

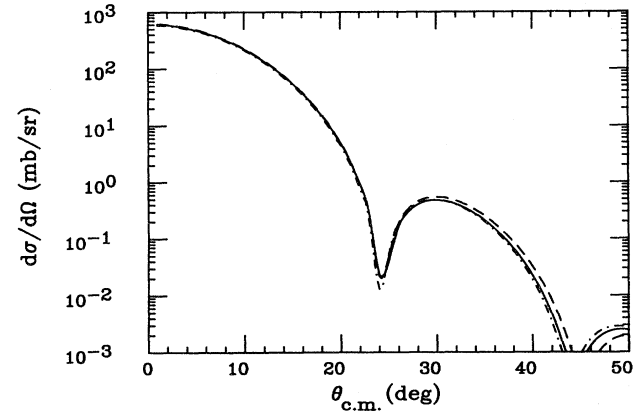

FIG. 3. Various approximations in the Glauber theory for π-^{12}C elastic scattering. The dashed curve is calculated using the Slater-determinant nuclear wave function [Eq. (8)] (the same as the dashed curve in Fig. 1), the solid curve using the product density [Eq. (10)], and the dot-dashed curve using the optical-limit expression [Eq. (12)]. These curves almost agree with each other.

B. Dependence on various effects in the πN scattering amplitudes

Since the Glauber theory is based on the on-mass-shell πN amplitudes, the agreement between the two formalisms discussed in Sec. III A implies that the off-shell effects of the πN amplitudes are negligible, at least in the elastic scattering.

In order to verify this expectation, we carry out an optical-potential calculation using different off-shell factors of the πN amplitudes. PIPIT3 is written to use different forms of the g function in Eq. (15): the Gaussian form, the Yukawa form, and $g(\kappa)=1$. We find that the different forms of the g functions yield practically the same π-^{12}C elastic-scattering cross section. The off-shell dependence is indeed weak, and we use the Gaussian form $g(\kappa)=\exp(-\kappa^2/\bar{\kappa}^2)$, where $\bar{\kappa}=4.1$ fm^{-1}, in the following calculation. Note that the situation is different in the Δ region: Some functional forms of the damping factor have been found to yield important effects [19].

There are two sets of the πN phase shifts available, obtained by Höhler [13] and by Cutkosky *et al.* [14]. We calculated the differential cross sections using both phase shifts in the lowest-order optical-potential model. The cross sections by the two sets of the phase shifts almost coincide with each other and differ by only a few percent around the maximum ($\approx 30°$). In the rest of our calculation, we use Höhler's phase shifts.

We also examine the effects of the πN spin- and isospin-flip amplitudes on the double-scattering contribution in an approximate way, neglecting the noncommutability of Γ's [see Eq. (8)]. The difference between the differential cross sections calculated with and without the spin-flip part in the πN scattering amplitudes is found to be within a few percent. We consider this result to be reasonable because the spin-flip amplitude vanishes in the forward direction and is smaller than the spin-nonflip amplitude in any angle. The nuclear form factor also suppresses the spin-flip contribution in large angles when the proper nuclear density is used. The configuration mixing within the ground-state wave function alters the result little since the mixing is negligible for high states and causes little change in the matrix elements of the Γ's for the neighboring states. An example of the latter case is a mixing from the $p_{1/2}$ state. (Note that for the second-order potential we examine in Sec. IV, all excited states are included through application of the closure, but we find the spin-flip contribution to be small.) Accordingly, we will neglect the spin-flip contribution in the following discussions. We find that the isospin-flip contribution is negligible as well, in agreement with Ref. [20], stemming from the smallness of the isovector amplitude in comparison to the isoscalar amplitude.

The nuclear-binding effect is known to be approximately accounted for by shifting the πN total energy [21]. Since 800 MeV/c is a little (by about 40 MeV/c or 40

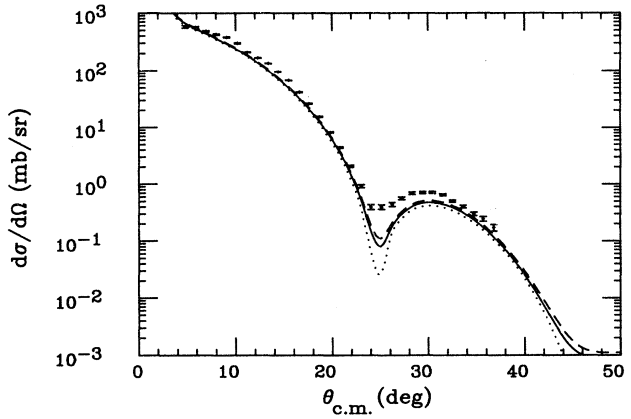

FIG. 4. Nuclear binding effect for π^+-^{12}C scattering. The optical-potential calculation at 800 MeV/c (solid curve, the same as the dotted curve of Fig. 1) is compared with those calculated by the use of the πN phase shifts at the energies shifted by 20 MeV (dotted curve) and by -20 MeV (dashed curve). The data are taken from Ref. [1].

MeV in the laboratory system) above the $N(1535)$, the effect of energy variation should be examined: We vary the energy of the πN amplitude used in the optical-potential model by ± 20 MeV (but keeping other kinematics the same) and find the corresponding variation in the differential cross sections to be small. Figure 4 illustrates this point.

C. Dependence on nuclear wave function

Within the HO wave function, we examine the dependence on various effects related to the nuclear wave function, using the Glauber theory.

(1) When the harmonic-oscillator parameter a_0 is varied, the position of the first minimum in the differential cross section changes, but importantly, the depth of the minimum does not change. As described in Sec. II, the value of a_0, which is actually used in our calculation, is chosen so as to fit high-energy electron-scattering data unfolding the nucleon charge form factor and including the c.m. correction. This choice turns out to be the optimum, giving the best agreement with the π-^{12}C differential cross sections.

(2) It is essential to unfold the nucleon form factor from the nuclear charge form factor. The differential cross sections differ appreciably without unfolding the nucleon form factor. The detailed functional form of the nucleon form factor is not, however, crucial as long as it gives the correct nucleon rms radius. We also confirm this point numerically with the optical-potential model using other functional forms of (linear) dipole and Gaussian.

(3) When the c.m. motion correction [the exponential factor in Eq. (4)] is removed, the cross sections change at large angles ($>20°$), as expected from the functional form. The change observed is significant: The c.m. correction is not merely a $1/A$ (about 8% here) correction, but has a strong momentum dependence. The correction must be included for the examination of large-angle scattering as in Refs. [20] and [22].

(4) The antisymmetrization (Pauli correlation) effect is found to be small as discussed in Sec. III A.

D. Comparison with the data

Figure 1 also shows comparison of the lowest-order calculation and the data. We see that the lowest-order theoretical calculation consistently underestimates the cross sections. The underestimation is over all the momentum range, amounts to 20–30 %, and is relatively larger with π^- scattering. Note that it occurs even in the forward angle, for which our formalisms should be particularly reliable. The amount of the underestimate is larger than the relative and normalization experimental uncertainties. The uncertainties explicitly shown in Fig. 1 are the relative uncertainties. The normalization uncertainty is reported to be about 15% [1].

This underestimation or the difference between the lowest-order calculation and the data could be removed, if we were to increase the magnitudes of the real and imaginary parts of the πN amplitude by 30% and 10%, respectively. We illustrate this point in Fig. 5.

On this point we are in agreement with recent works using the Glauber theory [20,22]. A technical note would be, however, needed here for comparison with other works: The authors of Ref. [22] previously carried out a Glauber calculation [12], which yielded a better agreement with the data than both ours and Ref. [22]. The better agreement is illusionary since Ref. [12] uses an improperly isospin-averaged πN amplitude in the approximate Gaussian form. The isospin dependence of the πN amplitudes is rather prominent around this energy, and the π-nucleus cross sections depend sensitively on the πN amplitudes. The treatment of the πN amplitudes requires

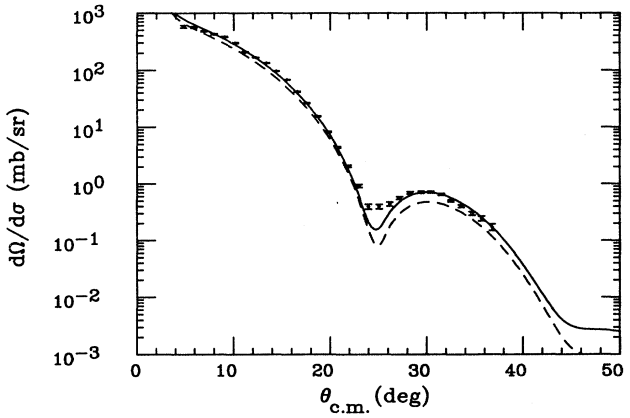

FIG. 5. Effect of an artificial modification of the πN amplitudes used in the optical-potential model. The dashed curve is the unmodified result (the same as the dotted curve in Fig. 1) for π^+-^{12}C scattering. The solid curve is the result of a modification by enlarging the real part of the isoscalar πN amplitude by 30% and the imaginary part by 10%. The data are taken from Ref. [1].

care for a serious comparison with the data. We emphasize here that in our work, the Höhler's partial-wave amplitudes are used as they are given, including their momentum dependence. The natural question then is whether the increase could be explained by higher-order effects. We address this question in the following section.

IV. HIGHER-ORDER EFFECTS

A. Nuclear correlation

So far, we have used the antisymmetrized, single-particle, nuclear wave function. We now examine the effect of dynamical correlation beyond the Pauli correlation. We will consider the two-nucleon correlation, which modifies the Glauber multiple-scattering series as well as the second-order optical potential.

It is straightforward to include the correlation function in the double-scattering term in the Glauber multiple-scattering series [Eq. (7)], but it rapidly becomes exceedingly complicated as the number of scattering increases. As demonstrated in Sec. III, the simple expression in the large-A limit without the antisymmetrization is a good approximation to the full Glauber theory. In order to simplify the calculation, we thus examine how the phase-shift function in this limit is modified by the two-nucleon correlation. That is, we calculate the second-order term, which is to be added to the first-order term of $\chi(\mathbf{b})$ in Eq. (12).

Up to the second-order term, the phase-shift function is then

$$\chi(\mathbf{b})\approx iA\int d^3r\,\Gamma(\mathbf{b}-\mathbf{s})\rho(\mathbf{r})-\frac{i}{2}A^2\int d^3r_1 d^3r_2[\rho(\mathbf{r}_1,\mathbf{r}_2)-\rho(\mathbf{r}_1)\rho(\mathbf{r}_2)]\Gamma(\mathbf{b}-\mathbf{s}_1)\Gamma(\mathbf{b}-\mathbf{s}_2)\ . \tag{19}$$

The second-order term in $\chi(\mathbf{b})$ is, in more detail,

$$-\frac{i}{2}A^2\left[\frac{1}{2\pi i\kappa}\right]^2\int d^3r_1 d^3r_2 d^2q_1 d^2q_2[\rho(\mathbf{r}_1,\mathbf{r}_2)-\rho(\mathbf{r}_1)\rho(\mathbf{r}_2)]e^{-i\mathbf{q}_1\cdot(\mathbf{b}-\mathbf{s}_1)-i\mathbf{q}_2\cdot(\mathbf{b}-\mathbf{s}_2)}f(q_1)f(q_2)\ . \tag{20}$$

Here $\rho(\mathbf{r}_1,\mathbf{r}_2)$ is the two-body density defined as

$$\rho(\mathbf{r}_1,\mathbf{r}_2)=\int d^3r_3\cdots d^3r_A|\psi_0(\mathbf{r}_1,\mathbf{r}_2,\ldots,\mathbf{r}_A)|^2\ , \tag{21}$$

and is approximately written as

$$\rho(\mathbf{r}_1,\mathbf{r}_2)=\rho(\mathbf{r}_1)\rho(\mathbf{r}_2)[1+\lambda(r)]\ , \tag{22}$$

where $\lambda(r)$ is the correlation function.

Our evaluation of the second-order term is rather elaborate in comparison to the well-known estimate [23],

$$i\chi(\mathbf{b})=i\frac{2\pi A}{\kappa}f(0)\int_{-\infty}^{\infty}dz\,\rho(\mathbf{b},z)+\left[\frac{2\pi A}{\kappa}f(0)\right]^2 l_c\int_{-\infty}^{\infty}dz\,\rho(\mathbf{b},z)^2\ , \tag{23}$$

where l_c is the correlation length defined as

$$l_c=-\int_0^{\infty}dr\,\lambda(r)\ . \tag{24}$$

This estimate assumes that l_c is much smaller than the nuclear radius and much larger than the πN interaction range. The second assumption is not fully satisfied in our case, l_c being, for example, 0.4 fm for the hard-core NN potential. Numerically, Eq. (23) yields larger values to the second term by 20% in the real part and by 10% in the imaginary part.

We evaluate Eq. (20) using the one-parameter Jastraw-type correlation function [24], for simplicity,

$$\lambda(|\mathbf{r}_1-\mathbf{r}_2|)=-\exp(-\Lambda|\mathbf{r}_1-\mathbf{r}_2|^2)\ . \tag{25}$$

Here Λ is the correlation range and is determined from the relation

$$l_c=\tfrac{1}{2}\sqrt{\pi/\Lambda}\ .$$

Though the actual calculation is carried out for various $\mathbf{q}_1$ and $\mathbf{q}_2$, we describe the calculation in the following, using the special case of $\mathbf{Q}=\mathbf{q}_1+\mathbf{q}_2=\mathbf{0}$ and $\rho(r)\propto\exp(-r^2/a^2)$ for the purpose of illustration. The integral of Eq. (20) becomes, in this case,

$$\int d^2q\,d^3r\,d^3R\,\exp\left[-\frac{1}{a^2}\left[2R^2+\frac{r^2}{2}\right]\right]\exp(-\Lambda r^2)e^{i\mathbf{q}\cdot\mathbf{s}}f(q)^2=\int d^2q\frac{1}{(1+2a^2\Lambda)^{3/2}}\exp\left[-\frac{a^2q^2}{2(1+2a^2\Lambda)}\right]f(q)^2\ , \tag{26}$$

where $\mathbf{r}=\mathbf{r}_1-\mathbf{r}_2$, $\mathbf{R}=(\mathbf{r}_1+\mathbf{r}_2)/2$, and $\mathbf{q}=(\mathbf{q}_1-\mathbf{q}_2)/2$. Since $f(q)$ is a polynomial of q^2, this integral is carried out as, for example, for the $2n$th power term,

$$\int d^2q \frac{1}{(1+2a^2\Lambda)^{3/2}} \exp\left[-\frac{a^2q^2}{2(1+2a^2\Lambda)}\right] q^{2n} \exp\left[-\frac{2q^2}{\tilde{k}^2}\right] = \pi n! \left[\frac{2\tilde{k}^2}{4(1+2a^2\Lambda)+a^2\tilde{k}^2}\right]^{n+1} (1+2a^2\Lambda)^{n-1/2} , \tag{27}$$

in which the off-shell correction of $f(q)$ is also included, using a Gaussian-form damping factor $\exp(-q^2/\tilde{k}^2)$. This factor comes from the g functions, which have been introduced in Sec. II B for the lowest-order optical potential:

$$f(q) \propto \frac{g(\kappa')g(\kappa_0)}{g(\kappa_0)^2} \langle \kappa_0' | \tilde{t}(e) | \kappa_0 \rangle .$$

Because $\mathbf{q}$ is perpendicular to the incident momentum κ_0, we have

$$\frac{g(\kappa')g(\kappa_0)}{g(\kappa_0)^2} = \exp\left[-\frac{1}{\tilde{k}^2}(\kappa'^2+\kappa_0^2-2\kappa_0^2)\right] = \exp\left[-\frac{q^2}{\tilde{k}^2}\right] . \tag{28}$$

A technical note: As discussed in Sec. III, the factor contributes little to the lowest-order calculation of the Glauber theory. The factor is used here to secure the convergence of the integral for the polynomial form of $f(q)$ that we have chosen.

Let us now turn to the discussion of the second-order optical potential. Under the closure approximation, the second-order optical potential is written as [5,25]

$$\begin{aligned}
\langle \mathbf{k}',0|V_{\rm opt}^{(2)}|\mathbf{k},0\rangle &= \sum_{n\neq 0} \int \frac{d^3p}{(2\pi)^3} \langle \mathbf{k}',0|V_{\rm opt}^{(1)}|\mathbf{p},n\rangle \frac{1}{E-\hat{H}+i\epsilon} \langle \mathbf{p},n|V_{\rm opt}^{(1)}|\mathbf{k},0\rangle \\
&\approx (A-1)^2 \int \frac{d^3p}{(2\pi)^3} \langle \mathbf{k}'|t(e)|\mathbf{p}\rangle \frac{1}{E-H+i\epsilon} \langle \mathbf{p}|t(e)|\mathbf{k}\rangle \\
&\quad \times \{\langle 0|\exp[-i(\mathbf{k}'-\mathbf{p})\cdot\mathbf{r}_1 - i(\mathbf{p}-\mathbf{k})\cdot\mathbf{r}_2]|0\rangle \\
&\quad - \langle 0|\exp[-i(\mathbf{k}'-\mathbf{p})\cdot\mathbf{r}_1]|0\rangle \langle 0|\exp[-i(\mathbf{p}-\mathbf{k})\cdot\mathbf{r}_2]|0\rangle\} \\
&= (A-1)^2 \int \frac{d^3p}{(2\pi)^3} \langle \mathbf{k}'|t(e)|\mathbf{p}\rangle \frac{C(\mathbf{k}'-\mathbf{p},\mathbf{p}-\mathbf{k})}{E-H+i\epsilon} \langle \mathbf{p}|t(e)|\mathbf{k}\rangle ,
\end{aligned} \tag{29}$$

where

$$C(\mathbf{q}_1,\mathbf{q}_2) = \int d^3r_1 d^3r_2 e^{-i\mathbf{q}_1\cdot\mathbf{r}_1 - i\mathbf{q}_2\cdot\mathbf{r}_2} [\rho(\mathbf{r}_1,\mathbf{r}_2) - \rho(\mathbf{r}_1)\rho(\mathbf{r}_2)] , \tag{30}$$

and $|n\rangle$ means the nuclear excited state where the ground state is assigned as 0, and we use Eq. (13) for the first-order optical potential. Here

$$H = m_A + m_\pi + K_A + K_\pi + \langle \epsilon \rangle + \langle V \rangle , \tag{31}$$

where K_A and K_π are the kinetic energies of the nucleus and pion, respectively, $\langle \epsilon \rangle$ is an average nuclear excitation energy, and $\langle V \rangle$ is an average interaction energy between the intermediate pion and excited nucleus. We can safely neglect $\langle \epsilon \rangle$ and $\langle V \rangle$ below, because their magnitudes are at most several tens of MeV, being far smaller than $K_A + K_\pi \approx 650$ MeV [26]. We confirmed this by varying $\langle \epsilon \rangle$ and $\langle V \rangle$ as energy-independent parameters. The optical potential up to second order is written as

$$\begin{aligned}
\langle \mathbf{k}',0|V_{\rm opt}|\mathbf{k},0\rangle &= \langle \mathbf{k}',0|V_{\rm opt}^{(1)}|\mathbf{k},0\rangle + \langle \mathbf{k}',0|V_{\rm opt}^{(2)}|\mathbf{k},0\rangle \\
&= (A-1)\tilde{\rho}(\mathbf{q}) \langle \mathbf{k}'|t(e)|\mathbf{k}\rangle + (A-1)^2 \int \frac{d^3p}{(2\pi)^3} \frac{\langle \mathbf{k}'|t(e)|\mathbf{p}\rangle \langle \mathbf{p}|t(e)|\mathbf{k}\rangle}{E-E_\pi(\mathbf{p})-E_A(\mathbf{p})+i\epsilon} C(\mathbf{k}'-\mathbf{p},\mathbf{p}-\mathbf{k}) ,
\end{aligned} \tag{32}$$

and we solve Eq. (13) by substituting Eq. (32) for $\langle \mathbf{k}',0|V_{\rm opt}^{(1)}|\mathbf{k},0\rangle$.

In order to reduce the Lippmann-Schwinger equation [Eq. (13)] to a one-dimensional integral equation, we write the second-order optical potential $\langle \mathbf{k}',0|V_{\rm opt}^{(2)}|\mathbf{k},0\rangle$ as in Eq. (18). The reduction to the one-dimensional integral equation requires many tedious integrations to be carried out. They can be separated into two groups, those associated with the calculation of $C(\mathbf{q}_1,\mathbf{q}_2)$ and those with the momentum integration of Eq. (32). Let us make brief comments on the two groups separately.

$C(\mathbf{q}_1,\mathbf{q}_2)$ can be analytically calculated with the modified harmonic-oscillator form of nuclear density $\rho(\mathbf{r})$. The variables of the integral are transformed from $(\mathbf{r}_1,\mathbf{r}_2)$ to $(\mathbf{r}_1-\mathbf{r}_2,(\mathbf{r}_1+\mathbf{r}_2)/2)$ with the momentum $(\mathbf{k}_1+\mathbf{k}_2,(\mathbf{k}_1-\mathbf{k}_2)/2)$; the only calculation we have to do is Gaussian integral. Essentially, $C(\mathbf{q}_1,\mathbf{q}_2)$ is a function of the momentum transfer to the target nucleus $|\mathbf{q}_1+\mathbf{q}_2| = |\mathbf{k}'-\mathbf{k}|$, which is fixed through the calculation, $|\mathbf{q}_1-\mathbf{q}_2| = |\mathbf{k}'+\mathbf{k}-2\mathbf{p}|$, and the angle between $\mathbf{k}'-\mathbf{k}$ and $\mathbf{p}$.

The integration of Eq. (32) is more complicated: Even

if we write $\langle \mathbf{k}'|t(e)|\mathbf{k}\rangle$ as a sum of the partial waves, the angle integral of d^3p cannot be carried out analytically because $C(\mathbf{q}_1,\mathbf{q}_2)$ is also dependent on these angles in a complex way, which is coming from the correlation function $\lambda(r)$. Numerical integration thus has to be done in three dimensions.

The resulting integral equation is solved using PIPIT3 as in the case of the lowest-order optical potential in Sec. II.

B. Pion absorption

There is neither a measurement nor a reliable microscopic calculation available on the π-absorption cross section on ^{12}C. Here we first estimate it semiphenomenologically, using the known absorption cross section on deuteron [27].

We assume the potential form for the pion absorption to be [28]

$$V^{\rm abs}(\mathbf{r})=\frac{2\pi}{\mu}B[\rho(\mathbf{r})]^2 , \tag{33}$$

where B is the absorption strength. It generally has a complex value, but we determine only the imaginary part for the purpose of estimation. μ is the reduced mass of the π-nucleus system,

$$\mu=\frac{(m_\pi^2+k^2)^{1/2}(m_A^2+k^2)^{1/2}}{(m_\pi^2+k^2)^{1/2}+(m_A^2+k^2)^{1/2}} , \tag{34}$$

where m_A and m_π are the nuclear and pion masses, respectively, and k is the pion momentum. The potential form of Eq. (33) is commonly used in low energies and is modeled on the basis of the following assumptions: (1) Two-nucleon absorption processes dominate the absorption. (2) The effect of the finite interaction range is negligible. (3) The spin-isospin dependence of absorption is neglected.

These assumptions are either realistic or numerically insignificant in low energies, but they, particularly (1) and (2), are certainly not expected to be so, at this high energy. Since the absorption cross section on the deuteron is experimentally observed to decrease rapidly as the pion energy increases [27], we first make a crude estimate such as the order-of-magnitude evaluation, by adapting Eq. (33) as an effective form. As will be discussed in Sec. IV C, we ensure that such a crude estimate is insensitive to the specific form of the absorption potential. If the estimate were to turn out to be appreciable, a more careful analysis would certainly have been required.

The operator form of Eq. (33) is written under the above assumptions as

$$\hat{V}^{\rm abs}=\frac{2\pi}{\mu}B\frac{2}{A(A-1)}\sum_{i<j}^{A}\delta^3(\mathbf{r}-\mathbf{r}_i)\delta^3(\mathbf{r}-\mathbf{r}_j) , \tag{35}$$

for large-A nuclei. For the deuteron, however, Eqs. (33) and (35) yield significantly different results, depending on how the c.m. motion is treated. Though none is completely satisfactory, we consider a direct application of Eq. (35) to be more appropriate. The absorption potential is then proportional to the central value of the deuteron density,

$$V^{\rm abs}(\mathbf{r})=\frac{2\pi}{\mu}B\delta^3(\mathbf{r})\rho(0) , \tag{36}$$

instead of Eq. (33). We use this potential together with the deuteron wave function, which incorporates the loosely bound structure as described in Appendix C.

The phenomenological value of B is then computed in the Born approximation from the total absorption cross section on the deuteron, $\sigma_{\rm abs}$, as

$$\sigma_{\rm abs}=\frac{4\pi}{k}{\rm Im}\left[\frac{-\mu}{2\pi}\int d^3r\, V^{\rm abs}(\mathbf{r})\right]$$
$$=-\frac{4\pi}{k}{\rm Im}B\,\rho(0) . \tag{37}$$

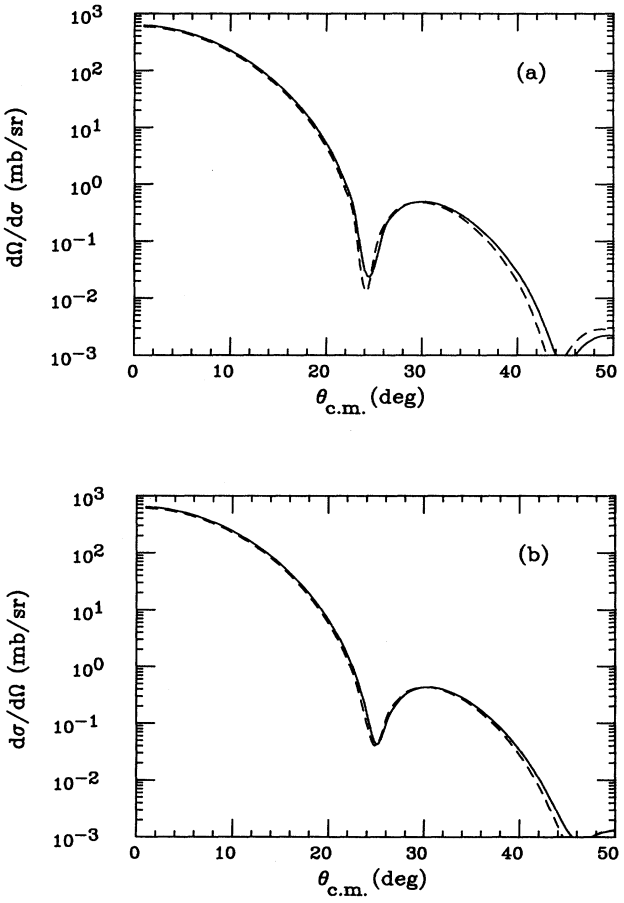

FIG. 6. (a) Effect of the nuclear correlation in the Glauber theory for π-^{12}C scattering. The dashed curve is without the nuclear correlation and the solid curve with the correlation using Eq. (20). (b) Effect of the nuclear correlation in the optical-potential model. The solid curve is calculated with the nuclear correlation using Eq. (32), and the dashed curve is without the correlation. The Coulomb interaction is not included for the sake of clarity. Note that the nucleon form factor is unfolded from the nuclear wave function only in the first-order optical potential (that is, the part of the calculation without the nuclear correlation).

C. Comparison with the data

Figure 6 shows the differential cross sections with and without nuclear correlation. We see that the difference between the two is slight; the correlation effect amounts to at most a few percent. Even if we use a large correlation range (~ 1.5 fm), the correlation effects enlarge the scattering amplitude less than 10%. The differential cross section becomes slightly large over the range we calculated. Our finding is in agreement with the general trend of this effect [4,23]. Below the Δ resonance, however, various correlations including the shell-model correlations have been noted to play an important role in charge-exchange processes [29].

In order to examine the π-absorption effect, we first compute B using the method described above, which yields $\mathrm{Im}B \approx -0.35$ fm^4 for the observed value of $\sigma_{\mathrm{abs}} \sim 0.2$ mb [27]. This value of B is actually too small to alter the lowest-order result of Sec. III. An order-of-magnitude larger value is needed to bring the lowest-order result close to the data. Figure 7 shows that a reasonable agreement could be reached if we were to use $B \approx 57 - i57$ fm^4.

We thus find that the contribution from π absorption is small. This finding is certainly model dependent and has some uncertainty. Our examination of various other models, however, shows that the contribution is consistently small, unless some drastic, often unphysical, assumptions are adapted.

Concluding this section, we find that the higher-order effects examined here amount to only a few percent enhancement in the cross section, as long as the realistic strength of the nuclear correlation and π absorption is used. The 20–30% discrepancy between the data and our calculations thus remains a puzzle. Note that the discrepancy persists when the 15% experimental uncertainty in normalization is also included.

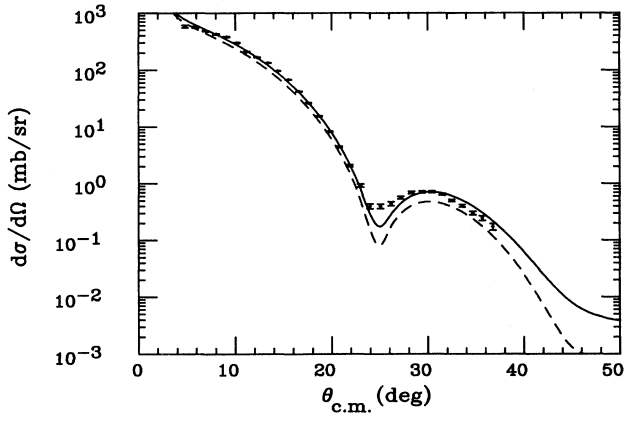

FIG. 7. Effect of the pion absorption. As the solid curve shows, a good agreement could be achieved if an unrealistically large value of $B = 57 - i57$ fm^4 should be used for π^+-^{12}C scattering. The dashed curve is the result of the first-order optical-potential model without the absorption (the same as the dotted curve in Fig. 1). The results are shown for π^+-^{12}C scattering. The data are taken from Ref. [1].

V. CHARGE-EXCHANGE REACTIONS

We have so far developed the Glauber theory sufficiently to carry out a simple estimate of charge-exchange reactions. Here we calculate the single- and double-charge exchange (SCX and DCX) reactions to the isobaric and double isobaric-analog states (IAS and DIAS, respectively) at 800 MeV/c: $^{13}\mathrm{C}(\pi^+,\pi^0)^{13}\mathrm{N}_{\mathrm{IAS}}$, $^{14}\mathrm{C}(\pi^+,\pi^0)^{14}\mathrm{N}_{\mathrm{IAS}}$, and $^{14}\mathrm{C}(\pi^+,\pi^-)^{14}\mathrm{O}_{\mathrm{DIAS}}$.

We emphasize that this calculation is not meant in any way to be the final one with the purpose of a serious prediction. The calculation is meant to be an attempt with the purpose of a simple estimate, which could be compared to more careful calculations so as to find the significance of various approximations made here. The charge-exchange reactions directly involve nuclear structure from the lowest-order process and have a promise of extracting useful structure information. In order to achieve this, we require a thorough understanding of (elastic-) scattering processes. As the reader can see after our discussions so far, however, our understanding has not reached this level. Note that though no charge-exchange-reaction data are available at this energy, they are now available up to 680 MeV/c [30].

In our calculation we make the following simplification: (1) Isobaric-analog states are taken to be the only intermediate states during the reactions, and the profile function is composed of the one-body operators as in Eq. (8). (2) The core (the nucleons in $s_{1/2}$ and $p_{3/2}$) is considered to be inert for the reactions, simply participating as the background. This simplification is tested by carrying out a cumbersome calculation using Eq. (7) in an approximate way, by switching on the charge-exchange processes in which the core is involved. We find the simplification to be well justified.

Our calculation thus involves 1 or 2 valence nucleons and 12 inner nucleons, the 2 groups of the nucleons having different roles. The scattering amplitude is written to reflect this as

$$G(\mathbf{Q}) = \frac{k}{2\pi i}\exp\left[\frac{Q^2 a_0^2}{4A}\right] \times \int d^2b\, e^{i\mathbf{b}\cdot\mathbf{Q}}\left[-\int \Gamma_{\mathrm{ex}}(\mathbf{b}-\mathbf{s})\rho_{\mathrm{v}}(\mathbf{r})d^3r\right]^n \times \exp[i\chi(\mathbf{b})]\ , \tag{38}$$

where $\chi(\mathbf{b})$ is the phase-shift function due to the π elastic scattering,

$$\exp[i\chi(\mathbf{b})] = \left[\int d^3r[1-\Gamma(\mathbf{b}-\mathbf{s})]\rho(\mathbf{r})\right]^{A-n}, \tag{39}$$

Γ_{ex} is the charge-exchange part of the profile function, $\rho_{\mathrm{v}}(\mathbf{r})$ is the density of valence nucleon, and n is 1 for SCX and 2 for DCX.

We use the formulation of Eqs. (38) and (39) because we find that the multiple-scattering series for the charge-exchange reactions do not converge at the fourth-scattering term at this energy. This simplified formulation is justifiable, since the multiple expansion of Eqs. (38) and (39) and the full Glauber multiple-scattering expan-

sion are found to yield practically the same numerical result, up to the fourth term.

For the elastic part $\chi(\mathbf{b})$, we use an averaged nuclear density for $\rho(r)$ and use the isoscalar parts for $\Gamma(\mathbf{b}-\mathbf{s})$. For the charge-exchange part, the isovector quantity Γ_{ex} must be treated with care for the double-charge-exchange reactions $n=2$. The schematic Γ^2 in Eq. (38) actually consists of two terms, being roughly

$$\theta(z_1-z_2)\Gamma_{ex}(\mathbf{b}-\mathbf{s}_1)\Gamma_{ex}(\mathbf{b}-\mathbf{s}_2) + \theta(z_2-z_1)\Gamma_{ex}(\mathbf{b}-\mathbf{s}_2)\Gamma_{ex}(\mathbf{b}-\mathbf{s}_1) ,$$

in the operator form. When this operator is evaluated for a double-charge-exchange process, we find a mere product of two Γ's, which we would have obtained without considering this subtlety.

The results for $^{14}C(\pi^+,\pi^0)^{14}N_{IAS}$ are shown in Fig. 8(a), and the results for $^{14}C(\pi^+,\pi^-)^{14}O_{DIAS}$ are in Fig. 8(b).

Closing this section, we make brief comments on possible improvement on our calculation, apart from better treatment of the simplification listed above. The choice of $\rho_v(\mathbf{r})$ deserves more care than our use of the HO density, since the cross sections are directly related to $\rho_v(\mathbf{r})$ as seen in Eq. (38). In addition, other channels of the double-charge-exchange process should be included such as the one through π^+-η-π^- because of the proximity to $N(1535)$, which has a large ηN decay width.

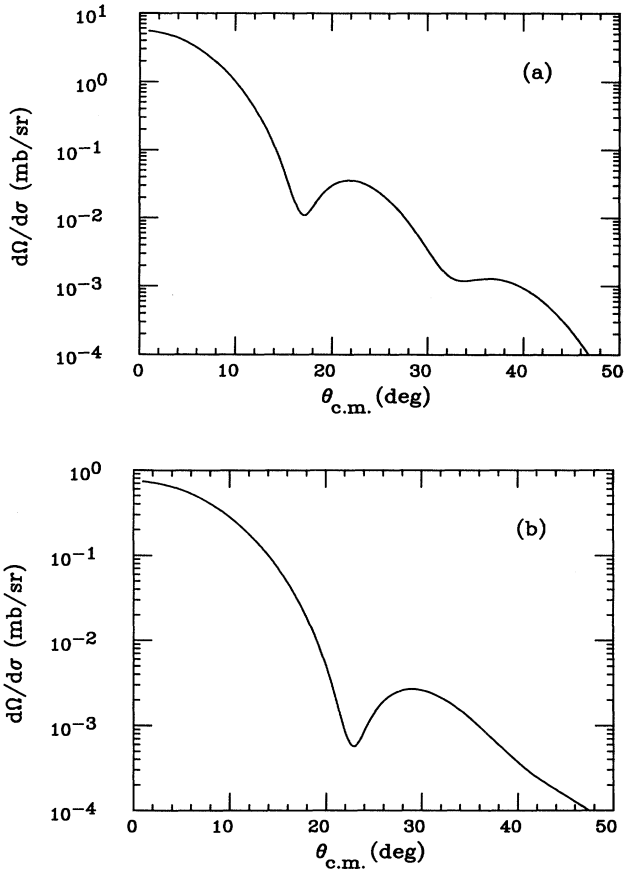

FIG. 8. (a) Single-charge-exchange cross sections for $^{14}C(\pi^+,\pi^0)^{14}N_{IAS}$ at 800 MeV/c. The cross sections are calculated using the Glauber theory [Eq. (38)]. Here the nucleon form factor is not unfolded, but the nuclear c.m. motion is corrected. (b) Double-charge-exchange cross sections for $^{14}C(\pi^+,\pi^-)^{14}O_{DIAS}$ at 800 MeV/c.

VI. SUMMARY AND DISCUSSION

We have investigated the elastic π-^{12}C scattering at 800 MeV/c by applying the two formalisms, the Glauber theory and the optical-potential model, which are based on the multiple-scattering expansion.

The two formalisms yield the elastic differential cross sections in agreement with each other, but in disagreement with the data. The disagreement amounts to 20–30 % by the first-order optical potential and Glauber theory calculations, as shown by other recent Glauber calculations [20,22]. Various corrections within the first-order potential, such as the spin-flip contribution in the πN amplitude, yield negligible contributions. The disagreement remains after the inclusion of the nuclear correlation and pion absorption in the second-order potential.

As an added exercise, we have also made a simple estimate of charged-exchange cross sections at this energy, which may be useful for comparison with more elaborate, future calculations.

In this work we have concentrated on the π-^{12}C scattering. Since the Brookhaven data also include scattering from ^{40}Ca, we have repeated the same calculations for the ^{40}Ca scattering as those for the ^{12}C, and have found that the results are remarkably the same. The disagreement is indeed common to scattering from both nuclei observed at this energy by the Brookhaven experiment.

In conclusion, the puzzling disagreement persists.

We plan to investigate the disagreement by examining other medium corrections beyond the pion absorption, which are not included in the multiple-scattering expansion in the original form. The medium corrections include those which stem from the bosonic nature of the pion at this high energy, such as pion production, and those which are generated by N^*- and Δ^*-resonance formation in nuclei. These are complicated processes of nonlocal nature. During the course of the examination, we expect to address the question of whether and to what degree the isobar-hole model is applicable here.

Before closing, let us discuss some aspects of the disagreement that offer a line of thought quite different from the above.

So far in this work, we have calculated the cross sections strictly at 800 MeV/c. The measurement of the 800 MeV/c differential cross sections is reported to have a 2.5% resolution in the incident momentum and a $\pm 0.5°$ angular uncertainty. This complication is found, however, to be of little consequence for the disagreement issue: Figure 9 illustrates the variations caused by the momentum resolution. Though the cross sections deviate by about 20% at the extreme ends of the momentum-

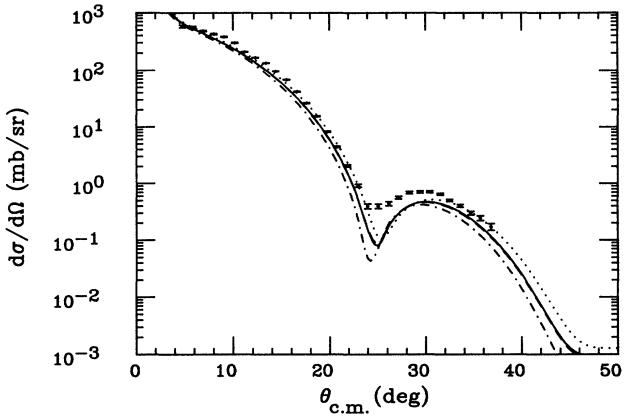

FIG. 9. Variation of the π^+-^{12}C differential cross sections, which is due to the pion-momentum resolution of $\pm 2.5\%$ and the angular uncertainty of the $\pm 0.5°$ in the measurement (Ref. [1]). The solid curve is calculated for 800 MeV/c (the same as the dotted curve in Fig. 1), the dot-dashed curve for the $+2.5\%$ excess momentum, and the dotted curve for the -2.5% excess momentum. The dashed curve is the average over the $\pm 2.5\%$ momentum region using the weight of the skewed Gaussian profile (Ref. [31]) observed in the experiment of Ref. [1], as well as the average over the angular uncertainty with the Gaussian weight. The dashed curve is very close to the solid curve and is hardly recognizable.

resolution range, their average comes very close to the calculated cross sections at 800 MeV/c. In fact, the difference between two curves is hardly recognizable in Fig. 9. The averaging is done with the weight of a skewed Gaussian, the incident momentum profile [31] in the original experiment of Ref. [1], as well as by taking account of the angular uncertainty with the Gaussian weight.

The disagreement similar to the one here has been reported for the K^+-nucleus scattering data at 800 MeV/c taken by the same experimental group [32]. Since K^+ is the weakest, strongly interacting probe and has no known resonance with the nucleon, such a discrepancy is difficult to explain by conventional physics. Some interesting explanations have been proposed, such as the swelling of nucleons and the variation of the ρ-meson mass in nuclei [33,34]. It is difficult to see whether such explanations could also be applicable to our pion case because the resonances and inelastic reactions cloud the issue.

As a speculative examination, however, we increased the nucleon size by 10% in the nucleon form factor upon unfolding, without altering the elementary πN amplitudes. The consequence of this increase was small: The change was invisible in the forward angle ($<25°$) and was only a few percent at larger angles. If the nucleon should swell, the πN amplitudes would be certainly modified. The modification in this case is more difficult to model than in the K^+N case. In order to examine the effect, we followed the idea of the ρ mass variation in Ref. [34]: We increased the background parts of the πN amplitudes after subtracting the resonance contributions (estimated in the Wigner form). We found that a reasonable agreement in the π-^{12}C differential cross sections could be obtained if we were to increase all πN partial waves. Such an increase corresponds to the drastic description that all of the background πN amplitudes are generated by the ρ exchange.

These examinations are not decisive, but it appears to us that the swelling nucleon and ρ-meson mass variation would be an unlikely possibility as the explanation of the discrepancy discussed here.

Recently, π-^{12}C differential cross sections have been measured at 400 and 500 MeV of the pion-laboratory energies [2]. We have extended our calculation to these energies and have found them in good agreement with the preliminary data. Our findings suggests either that the experimental calibration of the magnitude of the differential cross sections had been off or that highly energy-dependent physics is missing from our calculations.

ACKNOWLEDGMENTS

This work was partly carried out at Kellogg Radiation Laboratory, California Institute of Technology. M. A. acknowledges S. Koonin and other members of the Laboratory for their warm hospitality during his visit. We thank K. Yazaki, T. Nagae, H. Toki, and M. Mizoguchi for stimulating and helpful discussions. We also thank Particle Data Group for sending us the Höhler's and Cutkosky's πN phase shifts in a tabulated form, G. Burleson for data of the cross section at 400 and 500 MeV, and R. Chrien for the incident-pion momentum profile of the 800 MeV/c Brookhaven experiment. The final stage of this work was carried out at the LAMPF Theory Center: We (K.M. and R.S.) acknowledge W. Gibbs for providing a stimulating environment. This work was supported by the Grant-in-Aid of the Japanese Ministry of Education, Science and Culture, by the U. S. Department of Energy under Contract DE-FG03-87ER40347 at California State University, Northridge, and by the U.S. National Science Foundation under Grants PHY88-17296 and PHY86-04197 at Caltech.

APPENDIX A: πN SCATTERING AMPLITUDES

We outline here how we obtain the πN scattering amplitudes from phase shifts. The momentum-transfer dependence of the amplitude is also compared with that of the nuclear form factor.

The πN scattering amplitude $f(q)$ is written as a function of the c.m. scattering angle θ as

$$f(q)=\tilde{f}(1-q^2/2\kappa^2)=\tilde{f}(\cos\theta)\ , \tag{A1}$$

where q is the magnitude of the momentum transfer $\mathbf{q}$ and is related to the πN relative momentum κ and to θ as

$$q=2\kappa\sin\left[\frac{\theta}{2}\right]\ . \tag{A2}$$

The standard, angular-decomposition form of $\tilde{f}(\cos\theta)$ is

$$\tilde{f}(\cos\theta)=\frac{1}{\kappa}\sum_l [(l+1)T_l^+ + lT_l^-]P_l(\cos\theta) + i\sigma\cdot\mathbf{n}\frac{1}{\kappa}\sum_l (T_l^+ - T_l^-)P_l^1(\cos\theta) , \quad \text{(A3)}$$

where the first and second terms are the scalar and vector parts of the scattering amplitude, respectively, and P_l and P_l^1 are the Legendre and associated Legendre polynomials, respectively. $T_l^{\pm}$'s are written further in terms of the $I=\frac{1}{2}$ and $\frac{3}{2}$ amplitudes,

$$T_l^{\pm}=\tfrac{1}{3}(T_{l,1/2}^{\pm}+2T_{l,3/2}^{\pm})+\tau\cdot\mathbf{T}\tfrac{1}{3}(T_{l,3/2}^{\pm}-T_{l,1/2}^{\pm}) , \quad \text{(A4)}$$

where τ and $\mathbf{T}$ are the N and π isospins, respectively. For the energy that interests us, it is enough to include the partial waves up to the h wave ($l=5$).

In high-energy scattering, approximated forms of the elementary scattering amplitude are often used with a small number of parameters. A three-parameter Gaussian form

$$f(q)=\frac{i\kappa\sigma}{4\pi}(1-i\rho)\exp\left[-\frac{\beta^2 q^2}{2}\right] , \quad \text{(A5)}$$

is commonly used for the description of high-energy NN scattering amplitude. This has also been used for πN scattering [12,20,22]. It is simple and convenient, describing the essential feature of the forward-peaked, high-energy scattering.

The simple, approximated forms of the amplitude serves well in the energy region where the partial-wave decomposition is impractical because data are too scarce for the number of partial waves involved. In our problem two careful phase-shift analyses are available, and the number of the partial waves involved is relatively large, but not impractically large. Besides, in large angles, particularly at dips of differential cross sections, we would need accurate πN amplitudes to assess the physics properly. Accordingly, we decided to use the partial-wave decomposition so as not to overlook any feature off the forward scattering.

The use of the partial-wave decomposition effects a complicated momentum dependence in the optical potential. The only practical way is to solve equations in the momentum space, as we have done.

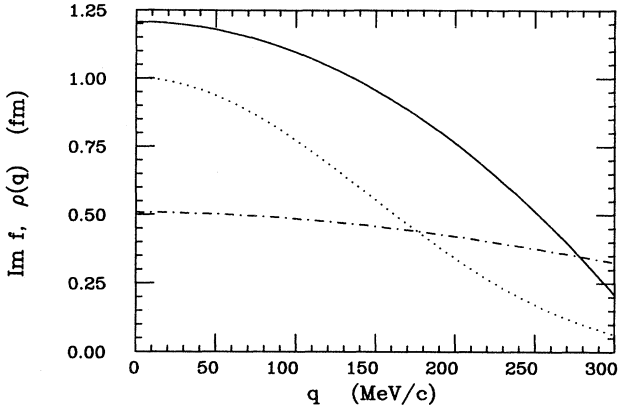

FIG. 10. Comparison of the πN scattering amplitude and the nuclear form factor as a function of the momentum transfer. The solid curve is the amplitude at 300 MeV/c pion momentum, the dot-dashed curve is at 800 MeV/c pion momentum, and the dotted curve is the nuclear form factor. The momentum transfer is measured in the pion-nucleus c.m. system. Note that for easy comparison, we omit the kinematic factors in the πN amplitudes arising from the coordinate transformations. The unit of the ordinate for the form factor is arbitrary.

Figure 10 illustrates the πN scattering amplitudes at 300 and 800 MeV/c as a function of momentum transfer. The forward peak at 800 MeV/c is seen to be much wider than the nuclear form factor, as is discussed in Sec. I, and also is seen to be wider than the peak at 300 MeV/c.

APPENDIX B: CORRECTION FOR NUCLEAR CENTER-OF-MASS MOTION IN THE GLAUBER THEORY

For completeness, we present a proof of Eq. (4), a consequence of nuclear center-of-mass correction in the Glauber theory [8].

We first construct the scattering amplitude, using the shell-model wave function analogous to Eq. (1) (but without the δ function). This scattering amplitude is expressed in terms of the coordinate system in which the shell-model potential is at the origin:

$$G_{\rm SM}(\mathbf{Q})=\frac{k}{2\pi i}\int d^2b' e^{i\mathbf{b}'\cdot\mathbf{Q}}\int d^3r_1'\cdots d^3r_A'\,\psi_{\rm SM}^{\dagger}(\mathbf{r}_1',\ldots,\mathbf{r}_A')\left[\prod_j^A [1-\Gamma(\mathbf{b}'-\mathbf{s}_j')]-1\right]\psi_{\rm SM}(\mathbf{r}_1',\ldots,\mathbf{r}_A') . \quad \text{(B1)}$$

Here $\mathbf{b}'=\mathbf{b}+\mathbf{S}$ and $\mathbf{s}_i'=\mathbf{s}_i+\mathbf{S}$, where $\mathbf{S}$ is a projection of the nuclear c.m. coordinate $\mathbf{R}$ on the plane perpendicular to $\mathbf{k}$. Note that $\mathbf{Q}\cdot\mathbf{R}=\mathbf{Q}\cdot\mathbf{S}$; $\mathbf{Q}$ and $\mathbf{k}$ are perpendicular to each other.

The use of the harmonic-oscillator (HO) wave functions enables us to write the nuclear, ground-state wave function as

$$\psi_{\rm SM}(\mathbf{r}_1',\ldots,\mathbf{r}_A')=\phi_{\rm c.m.}(\mathbf{R})\phi(\mathbf{r}_1,\ldots,\mathbf{r}_{A-1}) . \quad \text{(B2)}$$

Here the wave function is expressed as a product of two parts: $\phi_{\rm c.m.}(\mathbf{R})$ describing the c.m. motion and $\phi(\mathbf{r}_1,\ldots,\mathbf{r}_{A-1})$ describing the internal motion of the A nucleons. Note that $\mathbf{R}$ is measured with respect to the c.m. of the shell-model potential, and the $\mathbf{r}_i$'s are from $\mathbf{R}$. For the HO wave function

$$\phi(\mathbf{r}') \propto \exp\left[-\frac{r'^2}{2a_0^2}\right], \tag{B3}$$

the first factor is

$$\phi_{\text{c.m.}}(\mathbf{R}) \propto \exp\left[-\frac{AR^2}{2a_0^2}\right]. \tag{B4}$$

As they are defined above, the variables of the Γ function and thus the Γ function itself are invariant under the coordinate transformation, shifting the origin from the c.m. of the shell-model potential to the c.m. of the nucleus:

$$\Gamma(\mathbf{b}'-\mathbf{s}_i')=\Gamma(\mathbf{b}-\mathbf{s}_i). \tag{B5}$$

Putting them all together, Eq. (B1) is written as

$$\begin{aligned} G_{\text{SM}}(\mathbf{Q}) &= \frac{k}{2\pi i}\int d^2b \int d^3R\, d^3r_1 \cdots d^3r_{A-1} e^{i(\mathbf{b}+\mathbf{R})\cdot\mathbf{Q}} \phi^{\dagger}_{\text{c.m.}}(\mathbf{R})\psi^{\dagger}(\mathbf{r}_1,\ldots,\mathbf{r}_{A-1}) \\ &\quad \times \left[\prod_j^A [1-\Gamma(\mathbf{b}-\mathbf{s}_j)]-1\right]\phi_{\text{c.m.}}(\mathbf{R})\psi(\mathbf{r}_1,\ldots,\mathbf{r}_{A-1}) \\ &= \exp\left[-\frac{a_0^2Q^2}{4A}\right]\frac{k}{2\pi i}\int d^2b\, e^{i\mathbf{Q}\cdot\mathbf{b}} \int d^3r_1 \cdots d^3r_{A-1}\psi^{\dagger}(\mathbf{r}_1,\ldots,\mathbf{r}_{A-1}) \\ &\quad \times \left[\prod_j^A [1-\Gamma(\mathbf{b}-\mathbf{s}_j)]-1\right]\psi(\mathbf{r}_1,\ldots,\mathbf{r}_{A-1}) \\ &= \exp\left[-\frac{a_0^2Q^2}{4A}\right]\times[\text{Eq.}(1)], \end{aligned} \tag{B6}$$

where $\psi(\mathbf{r}_i,\ldots,\mathbf{r}_{A-1})$ includes the coordinate-transformation Jacobian from the $\{\mathbf{r}_i'\}$ coordinates to the $\{\mathbf{R},\mathbf{r}_i\}$ coordinates. Equation (B6) is the desired result.

APPENDIX C: AN ESTIMATE OF THE PION-ABSORPTION EFFECT

We estimate the pion-absorption strength parameter B using a deuteron wave function for the square-well potential whose depth and range, V_0 and a, are chosen to reproduce the binding energy of $W=2.2$ MeV. The wave function is

$$\psi(r)=\begin{cases} C_1 r^{-1}\sin(Kr)/\sqrt{4\pi}, & r\le a \\ C_2 r^{-1}\exp(-\gamma r)/\sqrt{4\pi}, & r>a \end{cases}, \tag{C1}$$

where C_1 and C_2 are normalization constants. K and γ are defined as $K=\sqrt{2m(V_0-W)}$ and $\gamma=\sqrt{2mW}$, and satisfy

$$\begin{aligned} &Ka\cot(Ka)=-\gamma a, \\ &C_1\exp(\gamma a)\sin(Ka)=C_2. \end{aligned} \tag{C2}$$

Here m is the reduced mass of the proton-neutron system. With the choice of $a=2.5$ fm and $V_0=0.13$ fm^{-1}, the normalization constants are $C_1=0.54$ and $C_2=0.92$. The density is given by

$$\rho(r)=|\psi(r)|^2. \tag{C3}$$

The pion-absorption cross section on deuteron σ_{abs} is observed to be about 0.2 mb [27], and then Eq. (37) with Eq. (C3) yields $\text{Im}B=-0.35$ fm^4.

[1] D. Marlow *et al.*, Phys. Rev. C **30**, 1662 (1984).
[2] LAMPF experiment No. 1106; G. Burleson (private communication).
[3] M. Arima and R. Seki, in *Proceedings of the 2nd LAMPF International Workshop on Pion-Nucleus Double Charge Exchange,* edited by W. R. Gibbs and M. J. Leitch (World Scientific, Singapore, 1990), p. 419.
[4] R. J. Glauber, in *Lectures in Theoretical Physics,* edited by W. E. Brittin and L. G. Dunham (Interscience, New York, 1959), Vol. I, p. 315; in *High Energy Physics and Nuclear Structure,* edited by G. Alexander (North-Holland, Amsterdam, 1967), p. 311; in *High Energy Physics and Nuclear Structure,* edited by S. Devons (Plenum, New York, 1970), p. 207. See also R. H. Bassel and C. Wilkin, Phys.

Rev. **174**, 1179 (1968).
[5] A. K. Kerman, H. McManus, and R. M. Thaler, Ann. Phys. (N.Y.) **8**, 551 (1959).
[6] J. M. Eisenberg and D. S. Koltun, *Theory of Meson Interactions with Nuclei* (Wiley, New York, 1980).
[7] V. Franco and R. J. Glauber, Phys. Rev. **142**, 1195 (1966).
[8] S. Gartenhaus and C. Schwartz, Phys. Rev. **108**, 482 (1957); W. Czyż, *Interactions of High-Energy Particles with Nuclei,* Nat. Bur. Stand. (U.S.) Monograph No. 139 (U.S. GPO, Washington, D.C., 1975).
[9] For example, see L. J. Tassie and F. C. Barker, Phys. Rev. **111**, 940 (1958).
[10] C. W. de Jager, H. de Vries, and C. de Vries, At. Data Nucl. Data Tables **14**, 479 (1974).
[11] W. S. C. Williams, *An Introduction to Elementary Particles* (Academic, New York, 1971), p. 451; R. A. Eisenstein and F. Tabakin, Phys. Rev. C **26**, 1 (1982).
[12] M. Mizoguchi *et al.*, Prog. Theor. Phys. **81**, 1217 (1989).
[13] G. Höhler, *Pion Nucleon Scattering,* Vol. I/9b2 of Landolt-Börnstein (Springer-Verlag, Berlin, 1983).
[14] R. E. Cutkosky, C. P. Forsyth, R. E. Hendrick, and R. L. Kelly, Phys. Rev. **20**, 2839 (1979).
[15] R. A. Eisenstein and F. Tabakin, Comput. Phys. Commun. **12**, 237 (1976).
[16] M. I. Haftel and F. Tabakin, Nucl. Phys. **A158**, 1 (1970).
[17] R. H. Landau, S. C. Phatak, and F. Tabakin, Ann. Phys. (N.Y.) **78**, 299 (1973).
[18] C. M. Vincent and S. C. Phatak, Phys. Rev. C **10**, 391 (1974).
[19] K. P. Lohs and V. B. Mandelzweig, Z. Phys. A **283**, 51 (1977).
[20] V. Franco and H. G. Schlaile, Phys. Rev. C **41**, 1075 (1990).
[21] R. H. Landau and A. W. Thomas, Nucl. Phys. **A302**, 461 (1978).
[22] M. Mizoguchi and H. Toki, Nucl. Phys. **A513**, 685 (1990).
[23] E. J. Moniz and G. D. Nixon, Ann. Phys. (N.Y.) **67**, 58 (1971).
[24] R. J. Jastraw, Phys. Rev. **98**, 1479 (1955).
[25] H. Feshbach, A. Gal, and J. Hüfner, Ann. Phys. (N.Y.) **66**, 20 (1971).
[26] G. A. Miller and J. E. Spencer, Ann. Phys. (N.Y.) **100**, 562 (1976); T. S. H. Lee and S. Chakravarti, Phys. Rev. C **16**, 273 (1977); M. Wakamatsu, Nucl. Phys. **A312**, 427 (1978).
[27] M. Akemoto *et al.*, Phys. Lett. **149B**, 321 (1984).
[28] M. Ericson and T. E. O. Ericson, Ann. Phys. (N.Y.) **36**, 323 (1966).
[29] W. B. Kaufmann and W. R. Gibbs, in *Proceedings of the 2nd LAMPF International Workshop on Pion-Nucleus Double Charge Exchange,* edited by W. R. Gibbs and M. J. Leitch (World Scientific, Singapore, 1990), p. 135.
[30] A. L. Williams *et al.*, Phys. Lett. B **216**, 11 (1989); A. Doron *et al.*, Phys. Rev. C **26**, 189 (1982).
[31] D. Marlow, Ph.D. thesis, Carnegie-Mellon University, 1984.
[32] D. Marlow *et al.*, Phys. Rev. C **25**, 2619 (1982).
[33] P. B. Siegel, W. B. Kaufmann, and W. R. Gibbs, Phys. Rev. C **31**, 2184 (1985).
[34] G. E. Brown, C. B. Dover, P. B. Siegel, and W. Weise, Phys. Rev. Lett. **60**, 2723 (1988).